

MIT Open Access Articles

Thermalizing and Damping in Structural Dynamics

The MIT Faculty has made this article openly available. **Please share** how this access benefits you. Your story matters.

Citation: Louhghalam, Arghavan, et al. "Thermalizing and Damping in Structural Dynamics." Journal of Applied Mechanics, vol. 85, no. 8, May 2018, p. 081001. © 2018 by ASME.

As Published: <http://dx.doi.org/10.1115/1.4040080>

Publisher: ASME International

Persistent URL: <http://hdl.handle.net/1721.1/117487>

Version: Final published version: final published article, as it appeared in a journal, conference proceedings, or other formally published context

Terms of Use: Article is made available in accordance with the publisher's policy and may be subject to US copyright law. Please refer to the publisher's site for terms of use.



Arghavan Louhghalam

Department of Civil and
Environmental Engineering,
University of Massachusetts Dartmouth,
285 Old Westport Rd,
Dartmouth, MA 02747
e-mail: arghavan.louhghalam@umassd.edu

Roland J.-M. Pellenq

Massachusetts Institute of Technology,
Department of Civil and
Environmental Engineering,
CNRS-MIT Joint Lab <MSE>2: Multiscale
Materials Science for Energy and Environment,
Cambridge, MA 02139
e-mail: pellenq@mit.edu

Franz-Josef Ulm¹

Professor
Department of Civil and
Environmental Engineering,
Massachusetts Institute of Technology,
Cambridge, MA 02139
e-mail: ulm@mit.edu

Thermalizing and Damping in Structural Dynamics

Structural damping, that is the presence of a velocity dependent dissipative term in the equation of motion, is rationalized as a thermalization process between a structure (here a beam) and an outside bath (understood in a broad sense as a system property). This is achieved via the introduction of the kinetic temperature of structures and formalized by means of an extended Lagrangian formulation of a structure in contact with an outside bath at a given temperature. Using the Nosé–Hoover thermostat, the heat exchange rate between structure and bath is identified as a mass damping coefficient, which evolves in time in function of the kinetic energy/temperature history exhibited by the structure. By way of application to a simple beam structure subjected to eigen-vibrations and dynamic buckling, commonality and differences of the Nosé–Hoover beam theory with constant mass damping models are shown, which permit a handshake between classical damping models and statistical mechanics–based thermalization models. The solid foundation of these thermalization models in statistical physics provides new insights into stability and instability for engineering structures. Specifically, since two systems are considered in (thermodynamic) equilibrium when they have the same temperature, we show in the case of dynamic buckling that a persistent steady-state difference in kinetic temperature between structure and bath is but indicative of the instability of the system. This shows that the kinetic temperature can serve as a structural order parameter to identify and comprehend failure of structures, possibly well beyond the elastic stability considered here. [DOI: 10.1115/1.4040080]

Keywords: structural dynamics, damping, Nosé–Hoover Bath, kinetic temperature, dynamic buckling

1 Introduction

Structural damping is one of the most complex systems' input parameters required for the design and operation of engineering structures. It is key for structural analysis of tall buildings characterized by slenderness and sensitivity to resonant wind effects, for which extensive experimental damping data makes it possible today to identify the critical role of structural damping in acceleration-based motion perception criteria (for a state-of-the-art review, see Ref. [1]). Structural damping is equally critical in seismic response analysis of cable-stayed bridges, but is clouded by the uncertainty on the actual damping capacity of such structures during strong motion response (see e.g., Ref. [2]). Similar uncertainties have haunted the design and operation of nuclear power plants ever since the introduction of damping in the structural analysis of primary and secondary systems in the mid1970s (see e.g., Ref. [3]).

From an engineering mechanics perspective, the difficulty of defining damping originates from the dissipative nature of damping, whether the damping is velocity—or displacement driven (for a comprehensive review of existing engineering damping models and methods of solution, see Ref. [4] and references cited herein). This means that a part of the kinetic energy is dissipated into heat form. This energy dissipation can originate from either the material scale or the system scale, which makes it difficult to clearly identify its very origin and capture it via material/constitutive or structural modeling.

From a statistical mechanics point of view, the problem of damping is slightly different, in the sense that the addition of a

dissipation term in the conservation of momentum evokes a shift from a microcanonical ensemble to a canonical ensemble (see e.g., Ref. [5]). In the first, given constant mass and volume of the structure, the energy is conserved, meaning that all changes in internal energy (including irreversible changes) translate directly into changes of kinetic energy. This microcanonical ensemble (or NVE-ensemble, where N stands for the number of mass points, V the volume, and E the energy) is the undamped system [6]. In contrast, in the canonical ensemble (or NVT ensemble, with T a temperature), the system of interest (here a structural system) is in contact with an outside “bath” at a prescribed temperature. The two systems (structure and bath) are said to be in equilibrium, when they have the same temperature. Otherwise said, the system of interest and the bath exchange heat in such a way that any change in internal energy due to deformation is compensated by both changes in kinetic energy and a dissipation term in the conservation of momentum that ensures that the system—after sufficiently long time—will ultimately reach the same temperature to be at equilibrium.

With this framework in mind, we employ some simple tools of statistical mechanics to revisit the concept of structural damping in structural dynamics. To this end, we introduce the kinetic temperature of structures as an order parameter to delineate the dynamic behavior of engineering structures. For background, the kinetic temperature originates from the kinetic theory of gases and is a classical quantity in molecular science to link the translational kinetic energy of particles to velocity distributions following a Maxwell–Boltzmann velocity distribution. In the absence of an actual temperature as a state variable in molecular dynamics, thermostats have been introduced that permit rescaling the kinetic energy to a sought value to achieve a temperature-controlled thermodynamic ensemble. Herein, we apply one of them, the so-called Nosé–Hoover thermostat [7–9], to some simple beam systems subject to dynamic bending and buckling. This

¹Corresponding author.

Contributed by the Applied Mechanics Division of ASME for publication in the JOURNAL OF APPLIED MECHANICS. Manuscript received April 17, 2018; final manuscript received April 17, 2018; published online May 10, 2018. Editor: Yonggang Huang.

Nosé–Hoover beam theory is first presented using classical tools of Lagrangian Mechanics, redefining mass damping as a transition from an NVE to an NVT ensemble. Rather than considering a constant structural damping, it is suggested that the kinetic temperature may serve as a powerful integrated order parameter to capture system related—in contrast to material related—energy dissipation in the linear and nonlinear dynamics response of structures, and it may serve as well as a quantitative means to identify instability of motions.

2 Nosé–Hoover Beam Theory

Consider a structure in the microcanonical ensemble: the mass is conserved ($N = \text{const}$), the system size is fixed ($V = \text{const}$), and the energy is conserved ($E = \text{const}$). In this ensemble, the Lagrangian of the structure (\mathcal{L}_S), that is, the difference between the structure's kinetic energy and its potential energy, entirely defines the location and the velocity of each and every mass point of the structure; that is, for instance for a continuous beam structure in two-dimensional bending (neglecting forces)

$$\mathcal{L}_S = \int_{(L)} \left(\frac{1}{2} \rho A \dot{w}^2 - \left(\frac{1}{2} EI (w'')^2 \right) \right) dx \quad (1)$$

where ρ is the density, A the beam section, EI the bending stiffness, and $\dot{w} = \partial w / \partial t$ and $w' = \partial w / \partial x$. Using classical Lagrangian mechanics, the Euler–Lagrange equation provides the classical form of the undamped equation of motion of a beam in the NVE–ensemble

$$\begin{aligned} -\frac{\partial}{\partial t} \left(\frac{\partial \mathcal{L}_S}{\partial \dot{w}} \right) + \frac{\partial^2}{\partial x^2} \left(\frac{\partial \mathcal{L}_S}{\partial w''} \right) &= 0 \\ \Downarrow \\ \rho A \ddot{w} + \frac{\partial^2}{\partial x^2} (EI w'') &= 0 \end{aligned} \quad (2)$$

In contrast, following the thermodynamic ensemble definition, a canonical ensemble consists of putting the structure in contact with an outside bath at some reference temperature T_∞ . The Lagrangian of this extended system is thus the sum of the Lagrangians of the structure and the bath

$$\mathcal{L} = \mathcal{L}_S + \mathcal{L}_{\text{Bath}} \quad (3)$$

The Lagrangian of the bath, i.e., the difference between the bath's kinetic and potential energy, needs to be specified and coupled to the Lagrangian of the structure. The consideration of a bath of fictitious mass $Q > 0$ is at the core of the Nosé–Hoover thermostat [7–9]: the bath thermalized at temperature T_∞ is characterized by its fictitious mass $Q > 0$ (of dimension $[Q] = \text{ML}^2$) and a velocity ξ (of dimension $[\xi] = \text{Time}^{-1}$) defining thus the kinetic energy as $1/2 Q \xi^2$. In addition, the potential energy of the bath is $RT_\infty \ln(s)$, i.e., defined by a uniform distribution through a generalized coordinate s (where R analogous to the gas constant is the product of the number of degrees-of-freedom and the Boltzmann constant); hence

$$\mathcal{L}_{\text{Bath}} = \frac{1}{2} Q \xi^2 - RT_\infty \ln(s) \quad (4)$$

where velocity ξ and generalized coordinate s are related by

$$\xi = \frac{ds}{d\tau}; \quad s = \frac{d\tau}{dt} \quad (5)$$

That is, s defines the stretch in time scale between the time of the bath, τ , and the structural time, t , whereas ξ specifies the heat exchange between structure and bath. If we note that the time derivatives are related by

$$\frac{\partial s}{\partial t} = \xi s; \quad \dot{w} = \frac{\partial w}{\partial \tau} s; \quad \ddot{w} = s \frac{\partial}{\partial \tau} \left(\frac{\partial w}{\partial \tau} s \right) = \left(s^2 \frac{\partial^2 w}{\partial \tau^2} + s \frac{\partial w}{\partial \tau} \xi \right) \quad (6)$$

we can rewrite the extended Lagrangian (3) of structure and bath as follows:

$$\mathcal{L} = \int_0^L \left(\frac{1}{2} \rho A s^2 \left(\frac{\partial w}{\partial \tau} \right)^2 - \frac{1}{2} EI \left(\frac{\partial^2 w}{\partial x^2} \right)^2 \right) dx + \frac{1}{2} Q \xi^2 - RT_\infty \ln(s) \quad (7)$$

The resulting Lagrangian has two variables, $w = w(x, \tau)$ and $s = s(\tau)$, and their derivatives. Two Euler–Lagrange equations provide access to the equations of motion. First, the Euler–Lagrange equation for the variable w reads

$$\begin{aligned} -\frac{\partial}{\partial \tau} \left(\frac{\partial \mathcal{L}}{\partial (\partial w / \partial \tau)} \right) + \frac{\partial^2}{\partial x^2} \left(\frac{\partial \mathcal{L}}{\partial w''} \right) &= 0 \\ \Downarrow \\ \rho A \left(s^2 \frac{\partial^2 w}{\partial \tau^2} + 2 \xi s \left(\frac{\partial w}{\partial \tau} \right) \right) + \frac{\partial^2}{\partial x^2} (EI w'') &= 0 \end{aligned} \quad (8)$$

Written herein in the extended time scale, a change in variables back to real time using relations (6) yields

$$\rho A (\ddot{w} + \xi \dot{w}) + \frac{\partial^2}{\partial x^2} (EI w'') = 0 \quad (9)$$

Second, the Euler–Lagrange equation for the Nosé–Hoover variable s and velocity $\xi = ds/d\tau$ permits identifying the rate equation of the exchange rate ξ specifying the heat exchange between the beam's kinetic energy and the water bath

$$\begin{aligned} \frac{\partial \mathcal{L}}{\partial s} - \frac{\partial}{\partial \tau} \left(\frac{\partial \mathcal{L}}{\partial \xi} \right) &= 0 \\ \Downarrow \\ \int_{(L)} \left(\rho A s \left(\frac{\partial w}{\partial \tau} \right)^2 \right) dx - \frac{1}{s} RT_\infty - Q \frac{\partial \xi}{\partial \tau} &= 0 \end{aligned} \quad (10)$$

From Eq. (9), the Nosé–Hoover beam is recognized as nothing but a mass damped system (with $\rho A \xi \dot{w}$ a friction force density due to the contact with the bath), in which the mass damping coefficient ξ evolves according to Eq. (10), which can be rewritten—in real time—as a rate equation

$$\dot{\xi} = \frac{d}{dt} \left(\frac{\partial \ln(s)}{\partial t} \right) = s \left(\frac{\partial^2 s}{\partial \tau^2} \right) \equiv \frac{RT_\infty}{Q} \left(\frac{T(t)}{T_\infty} - 1 \right) \quad (11)$$

where $T(t)/T_\infty$ is the normalized kinetic temperature evolution

$$\frac{T(t)}{T_\infty} = \frac{1}{RT_\infty} \int_{(L)} \left(\rho A \left(\frac{\partial w}{\partial t} \right)^2 \right) dx \quad (12)$$

Thus far, as $T(t)/T_\infty \rightarrow 1$, the mass damping coefficient ξ is constant, signaling the attainment of equilibrium. Similarly, if Q is large, the damping coefficient evolves little, which corresponds to the case of a constant mass damping as employed in classical structural dynamics.

The thermalizing of the beam structure by means of a Nosé–Hoover thermostat can be easily extended to nonlinear phenomena originating both from geometric nonlinearities and material nonlinearities. To illustrate these extensions consider for instance, in the expression of the beam's Lagrangian, the

second-order term due to the action of a compressive axial force $P > 0$ [10]

$$\mathcal{L}_S = \int_{(L)} \left(\frac{1}{2} \rho A (\dot{w})^2 - \frac{1}{2} \left(EI (w'')^2 - P (w')^2 \right) \right) dx \quad (13)$$

Employing the Nosé–Hoover extended system description, one thus arrives at the classical equation of motion of dynamic buckling (see e.g., Ref. [11]) save an added damping term

$$\rho A (\ddot{w} + \zeta \dot{w}) + \frac{\partial^2}{\partial x^2} (EI w'') + \frac{\partial}{\partial x} (P w') = 0 \quad (14)$$

The damping coefficient ζ still evolves with Eq. (11). Yet, as the additional second-order term in Eq. (13) reduces de facto the potential energy, the presence of a compressive axial force is expected to increase the kinetic energy, and hence the kinetic temperature and as a consequence the heat exchange between bath and beam, that is, the damping coefficient ζ . A similar trend is to be expected if damage occurred along the beam system, reducing irreversibly the bending stiffness EI of the beam. There exists thus an intricate interplay—in time and space—between system damping and geometric and material nonlinearities, which is not captured by classical constant structural damping models.

3 Applications

For the purpose of illustration, consider a simply supported beam subjected to eigen-vibrations. In the first example, we observe the difference between classical damping models and the Nosé–Hoover thermostat. In the second example, the dynamic buckling of the beam is investigated.

3.1 Thermalizing Eigen-Vibrations. Consider thus a simply supported beam of length L , constant beam bending stiffness EI , and mass per unit length ρA . For the purpose of illustration, we are interested in the damping of eigen-vibrations—achieved here by considering an initial velocity V_0 along the beam length. The rational of imposing a constant initial velocity field is that it is expected to activate equally all eigenmodes in the system.

For the problem in hand, the equation of motion is given by Eq. (9), which we rewrite in dimensionless form $\bar{w} = w(\omega_0/V_0)$ and coordinates $\bar{x} = x/L$ and $\bar{t} = t\omega_0$ with $\omega_0 = \sqrt{EI/(\rho AL^4)}$, while considering a damping ratio $\zeta = \zeta/(2\pi^2\omega_0)$

$$\frac{\partial^2 \bar{w}}{\partial \bar{t}^2} + 2\pi^2 \zeta(\bar{t}) \frac{\partial \bar{w}}{\partial \bar{t}} + \frac{\partial^4 \bar{w}}{\partial \bar{x}^4} = 0 \quad (15)$$

together with the initial conditions

$$\bar{w}(\bar{x}, \bar{t} = 0) = 0; \quad \frac{\partial \bar{w}}{\partial \bar{t}}(\bar{x} \setminus (0, 1), \bar{t} = 0) = 1 \quad (16)$$

Similarly, the Nosé–Hoover thermostat Eq. (11) is rewritten in a dimensionless form using the damping ratio ζ instead of mass damping coefficient ζ

$$\frac{d\zeta}{d\bar{t}} = \frac{\Gamma}{2\pi^2} \left(\frac{T(\bar{t})}{T_0} - \frac{T_\infty}{T_0} \right); \quad \Gamma = \frac{\rho AL}{Q/L^2} \times \frac{RT_0}{EI/L} \quad (17)$$

together with the initial conditions, considering Eq. (17) for the evaluation of the initial kinetic temperature (12)

$$\zeta(\bar{t} = 0) = \zeta_0; \quad \frac{d\zeta}{d\bar{t}}(\bar{t} = 0) = \frac{\Gamma}{2\pi^2} \left(1 - \frac{T_\infty}{T_0} \right); \quad \frac{T_\infty}{T_0} = \frac{RT_\infty}{(\rho AL)V_0^2} \quad (18)$$

There are thus two dimensionless quantities required to solve for the eigen-vibration damping. One is the temperature ratio T_∞/T_0

between the bath and the beam, which for free vibrations is $T_\infty/T_0 \rightarrow 0$. In fact, a nonzero value for T_∞/T_0 would imply a residual kinetic energy in the system, with fluctuations around the mean kinetic energy defined by $T_\infty/T_0 > 0$. The second is the beam-to-water mass ratio captured by the kinetic coefficient Γ . Indeed, noting that ρAL is the mass of the beam, and Q/L^2 the mass of the (hypothetical) water bath, it is readily recognized from Eq. (17) that a constant damping ratio, $\zeta(\bar{t} = 0) \rightarrow \zeta_0$, for a beam with finite bending energy ($\sim EI/L$) compared to its initial kinetic energy ($1/2RT_0 = \frac{1}{2}(\rho AL)V_0^2$), refers to a vanishing beam-to-water bath mass ratio, $\Gamma \rightarrow 0$. In return, as Γ increases, the damping ratio evolves in time, due to the evolution of the kinetic energy of the beam compared to its initial kinetic energy

$$\frac{d\zeta}{d\bar{t}} = \frac{\Gamma}{2\pi^2} \frac{T(\bar{t})}{T_0}; \quad \frac{T(\bar{t})}{T_0} = \int_0^1 \left(\left(\frac{\partial \bar{w}}{\partial \bar{t}} \right)^2 \right) d\bar{x} \quad (19)$$

To illustrate this effect, we solve the system of equation in generalized coordinates, $\phi_n(\bar{x})$ and $\bar{q}_n(\bar{t})$, separating time from space, i.e., $\bar{w} = \sum_{n=1}^\infty \phi_n(\bar{x}) \bar{q}_n(\bar{t})$ with $\phi_n(\bar{x}) = \sin(n\pi\bar{x})$ for the simply supported beam; that is (see Appendix for a derivation using the extended Lagrangian formulation)

$$\left. \begin{aligned} \sum_{n=1}^\infty \left(\frac{d^2 \bar{q}_n}{d\bar{t}^2} + 2\pi^2 \zeta(\bar{t}) \frac{d\bar{q}_n}{d\bar{t}} + (n\pi)^4 \bar{q}_n(\bar{t}) \right) \phi_n(s) &= 0 \\ \frac{d\zeta}{d\bar{t}} &= \frac{\Gamma}{2\pi^2} \frac{T(\bar{t})}{T_0}; \quad \frac{T(\bar{t})}{T_0} = \frac{1}{2} \sum_{n=1}^\infty \left(\frac{d\bar{q}_n}{d\bar{t}} \right)^2 \\ \bar{q}_n(0) &= 0; \quad \frac{d\bar{q}_n}{d\bar{t}}(0) = \frac{4 \sin^2(n\pi/2)}{n\pi}; \quad \zeta(0) = \zeta_0 \end{aligned} \right\} \quad (20)$$

The nonlinearity induced by a time-history damping $\zeta(\bar{t})$ requires time integration for the solution of the coupled system of Eq. (20), but does not interfere with the generalized coordinate solution defined by Eq. (20). The time integration scheme is also specified in Appendix.

Figure 1 displays the evolution in time of the kinetic temperature $T(\bar{t})/T_0$ for different values of the beam-to-bath mass ratio Γ , with the evolution of the damping coefficient $\zeta(\bar{t})$ shown in a normalized plot in Fig. 2. The two figures illustrate the role of the water bath mass on the time scale of damping of the kinetic energy; herein illustrated in form of the kinetic temperature $T(\bar{t})/T_0$. That is, the kinetic energy associated with eigen-vibrations is dissipated the faster the greater the water-to-beam mass ratio; i.e., $t \sim 1/\sqrt{\Gamma}$. As a consequence, the damping coefficient, which expresses but the heat exchange rate between beam and bath (see Eq. (5)), scales as $\zeta \sim \sqrt{\Gamma}$.

These Nosé–Hoover beam results need to be compared with the evolution of the kinetic temperature for different constant damping ratios, $\zeta(\bar{t}) = \zeta_0$ obtained with $\Gamma = 0$, and shown in Fig. 3. The values herein employed for ζ_0 were determined so to match asymptotically the values obtained for the different Γ -values, that is, $\zeta_0 = \sqrt{\Gamma/(2\pi^2)}$ (see Fig. 2). It is thus not surprising that the dissipation rate for constant damping ratios (Fig. 3) is faster than the one predicted by the Nosé–Hoover thermostat (Fig. 1). Following the fluctuation–dissipation theorem of statistical physics, we mean by dissipation the difference between the initial total energy of the beam, $\mathcal{E}(0) = E_k(0)$, and the total energy of the beam at time t , $\mathcal{E}(t)$ —the difference being the amount of energy pumped out (or added to) the system due to the (frictional damping) contact of the beam with the bath; that is—in a dimensionless form

$$\bar{D}(\bar{t}) = \frac{D(\bar{t})}{E_{kin}(0)} = 1 - \frac{E_k(\bar{t})}{E_k(0)} - \frac{U(\bar{t})}{E_k(0)} \quad (21)$$

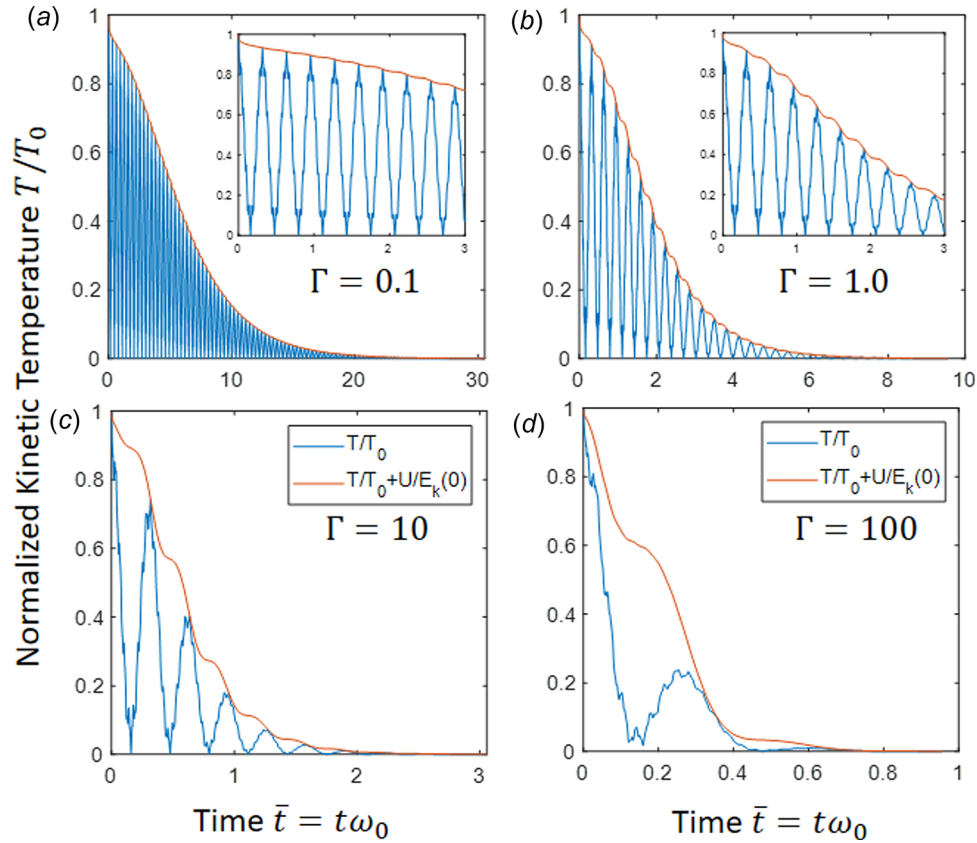


Fig. 1 Eigen-vibration dissipation of a simply supported beam obtained with a Nosé–Hoover thermostat. (a)–(d) Kinetic temperature evolution, $T(t)/T_0$, versus dimensionless time, $\bar{t} = t\omega_0$, for different beam-to-water mass ratios, $\Gamma = 0.1; 1; 10; 100$. [$\omega_0 = \sqrt{EI/(\rho AL^4)}$, with EI = beam bending stiffness, ρA = linear beam mass, L = beam length].

where $E_k(\bar{t})/E_k(0) = T(\bar{t})/T_0$ is the normalized kinetic energy evolution and $U(\bar{t})/E_k(0)$ is the normalized internal energy which is readily evaluated from Eq. (1) using generalized coordinates from relations Eq. (20)

$$\frac{U(\bar{t})}{E_k(0)} = \frac{1}{E_k(0)} \int_{(L)} \frac{1}{2} EI (w'')^2 dx = \frac{1}{2} \sum_{n=1}^{\infty} (n\pi)^4 \bar{q}_n^2 \quad (22)$$

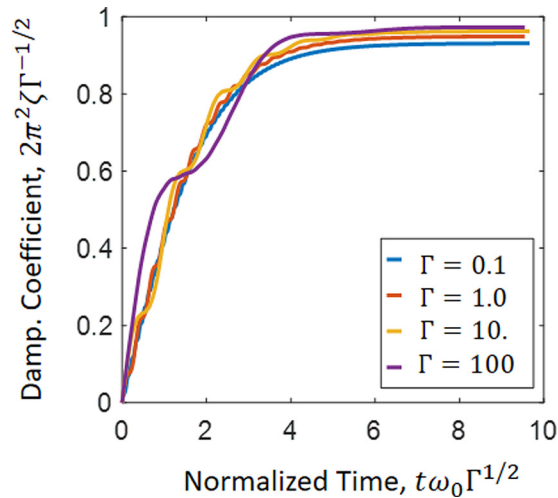


Fig. 2 Master-curve of the evolution in time of the damping coefficient predicted by the Nosé–Hoover beam theory for dissipating eigen-vibrations

This internal energy is displayed in Figs. 1 and 3, as the complementary part to the kinetic temperature. In Fig. 4, we compare the evolution of the dimensionless dissipation \bar{D} for the Nosé–Hoover thermostat (Fig. 4(a)) and for the classical constant mass damping model (Fig. 4(b)). The results indicate that by rescaling the time in the form $t\omega_0\Gamma^{1/2}$ and $t\omega_0(2\pi^2\zeta_0)$, respectively, a master-curve for the overall energy dissipation is obtained that is (almost) independent of the beam-to-water bath mass ratio, Γ , and the damping coefficient, ζ_0 . There are some differences in the specific evolution of \bar{D} , specifically in the characteristic time scale of the dissipation which is on the order of $t_c\omega_0\Gamma^{1/2} \approx 6$ for the Nosé–Hoover thermostat, and $t_c\omega_0(2\pi^2\zeta_0) \approx 4$ for the constant mass damping model.

In return, the overall consistency of the eigen-vibration dissipation between the two models lends a new meaning to structural damping models. Rather than being associated with some unknown dissipative sources, the Nosé–Hoover model defines damping from the heat exchange with an outside source that has (unlimited) access to all mass points in the system. Thus, instead of defining a single damping coefficient for capturing structural damping, the Nosé–Hoover thermostat defines the damping intensity by means of a single parameter, the beam-to-water mass ratio, Γ ; with bath being understood in a broad sense, as an outside thermalization source that pumps kinetic energy from or into the system.

This consistency permits us to use the scaling relations shown in Fig. 2 to make the handshake with structural damping ratios, ζ_m , for specific materials and structures reported in the literature (see e.g., Refs. [1–3]), using in a first approach $\Gamma_{eq} = (2\pi^2)^2\zeta_m$. Furthermore, the handshake with these classical models highlights the need for further refinements of the theory to account for e.g.,

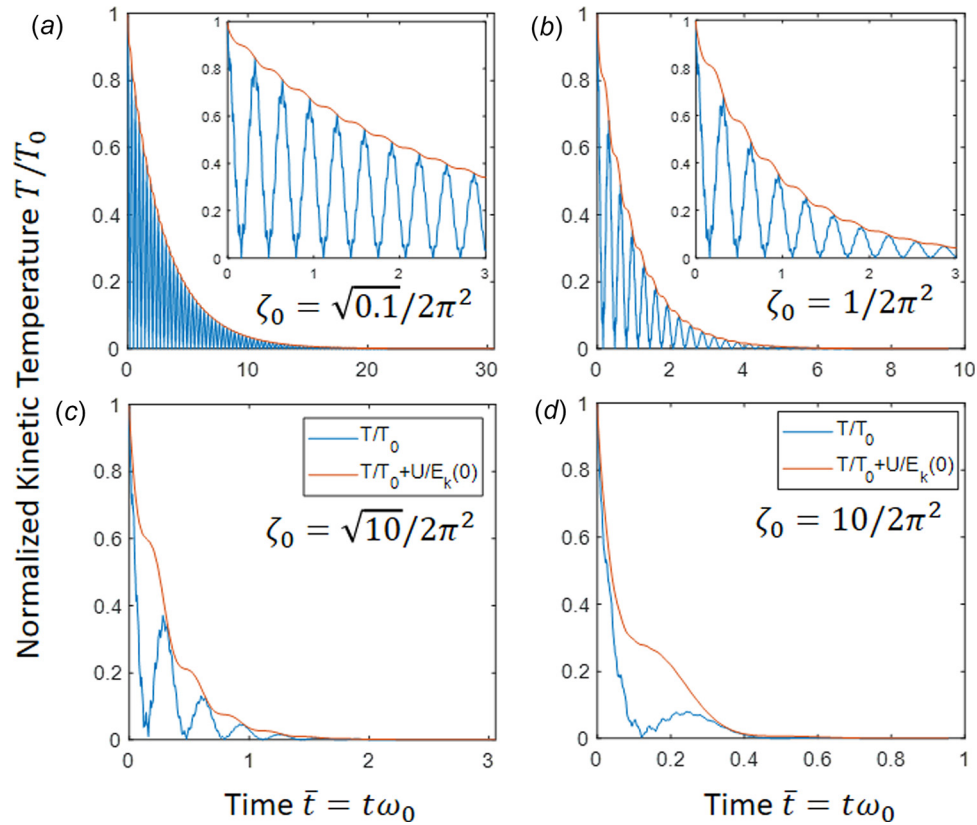


Fig. 3 Eigen-vibration dissipation of a simply supported beam obtained with the classical constant mass damping model. (a)–(d) Kinetic Temperature evolution, $T(\bar{t})/T_0$, versus dimensionless time, $\bar{t} = t\omega_0$, for different damping coefficients $\zeta_0 = \sqrt{\Gamma}/(2\pi^2)$ corresponding to beam-to-water mass ratios of $\Gamma = 0.1; 1; 10; 100$. [$\omega_0 = \sqrt{EI/(\rho AL^4)}$, with EI = beam bending stiffness, ρA = linear beam mass, L = beam length].

height-dependent damping ratios frequently employed in structural dynamics of tall buildings (see Ref. [1] and references cited herein). Such a height dependence can be taken into account by a height-dependent thermalization, that is, a series of Nosé–Hoover thermostats in parallel. All what it takes then is to properly rewrite the Lagrangians for different floors following the same procedure outlined here.

3.2 Decelerating Dynamic Buckling. The second example we consider is the case of dynamic buckling of a simply supported beam of length L . A classical textbook example, dynamic buckling is produced by an impulse generated by a mass M at speed U_0 at one end of the bar. This impulse puts in motion an axial wave that travels at the speed of sound, $c = \sqrt{E/\rho}$, along the beam and which is reflected at the end [12]. Provided that the time scale of

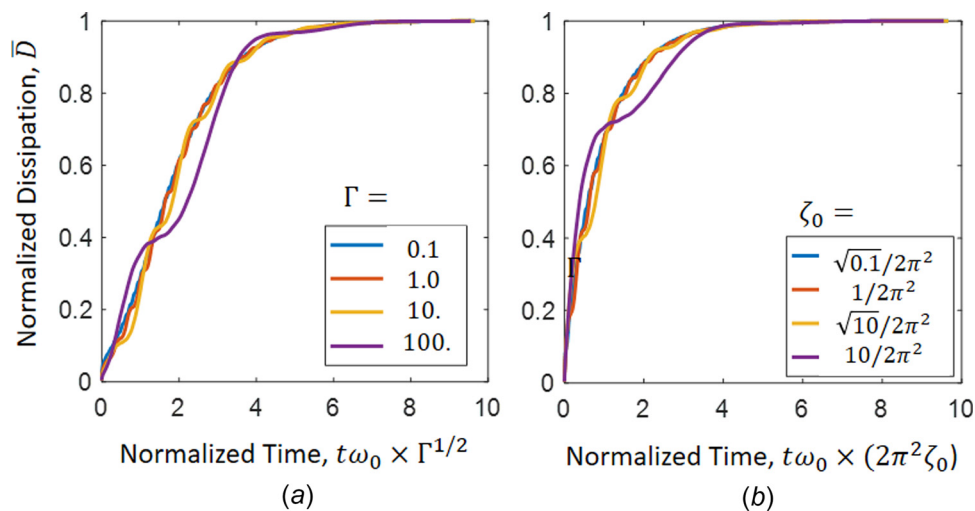


Fig. 4 Master-curves of eigen-vibration dissipation of a simply supported beam predicted by (a) the Nosé–Hoover thermalization model, and (b) the classical constant mass damping model

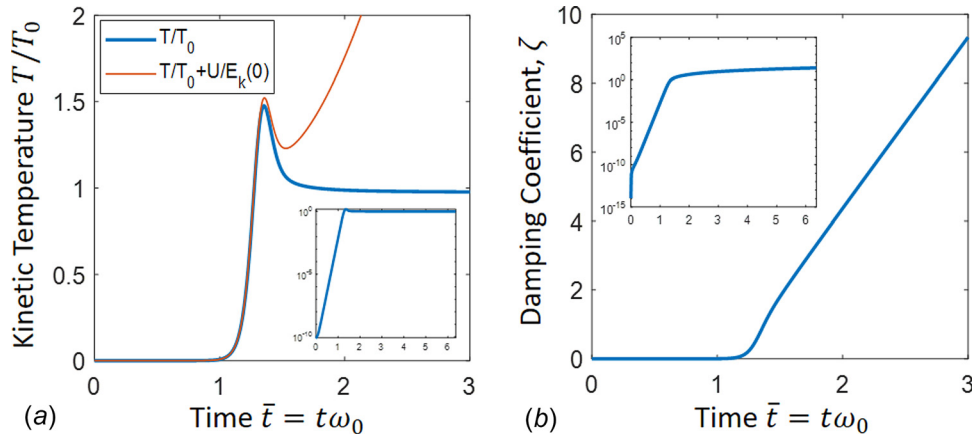


Fig. 5 Dynamic buckling: (a) kinetic temperature evolution $T(\bar{t})/T_0$ and internal energy evolution $T(\bar{t})/T_0 + U(\bar{t})/E_k(0)$ and (b) damping coefficient (results for $P = 2$; $\Gamma = 100$)

lateral vibration is much larger than the time scale of wave propagation along the beam, load P can be considered as constant along the beam length

$$P \simeq (1 + \gamma)EA \frac{U_0}{c} \quad (23)$$

with γ the number of reflections. For this case, the momentum balance (14) is written in the dimensionless form

$$\frac{\partial^2 \bar{w}}{\partial \bar{t}^2} + 2\pi^2 \zeta(\bar{t}) \frac{\partial \bar{w}}{\partial \bar{t}} + \frac{\partial^4 \bar{w}}{\partial \bar{x}^4} + \pi^2 \bar{P} \frac{\partial^2 \bar{w}}{\partial \bar{x}^2} = 0 \quad (24)$$

with

$$\begin{aligned} \bar{w} &= \frac{\omega_0}{U_0} \sqrt{\frac{\rho AL}{M}} w = \beta_s \frac{c}{U_0} \sqrt{\frac{\rho A}{ML}} w; & \bar{t} &= t\omega_0; \\ \bar{x} &= \frac{x}{L}; & \bar{P} &= \frac{P}{\pi^2 EI/L^2} \end{aligned} \quad (25)$$

Herein, $\omega_0 = \sqrt{EI/(\rho AL^4)}$, while $\beta_s = \sqrt{I/A}/L = \omega_0 L/c$ is the normalized radius of gyration of the beam. We introduce some initial perturbations in the system by considering an initial lateral velocity, V_0 , much smaller than the impact velocity so that the overall initial kinetic energy of the system is $E_k(0) = \frac{1}{2} MU_0^2 (1 + \epsilon^2)$, with $\epsilon = V_0/U_0 \times \sqrt{\rho AL/M} \ll 1$. The kinetic temperature after impact thus develops as:

$$\frac{T(\bar{t})}{T_0} = \frac{E_k(\bar{t})}{E_k(0)} = \frac{1}{(1 + \epsilon^2)} \int_0^1 \left(\frac{\partial \bar{w}}{\partial \bar{t}} \right)^2 d\bar{x} \quad (26)$$

which permits evaluating the Nosé–Hoover thermostat heat exchange rate

$$\frac{d\zeta}{d\bar{t}} = \frac{\Gamma}{2\pi^2} \left(\frac{T(\bar{t})}{T_0} - \frac{T_\infty}{T_0} \right); \quad \Gamma = \frac{\rho AL}{Q/L^2} \times \frac{MU_0^2}{EI/L} \quad (27)$$

where we considered $RT_0 = 2E_k(0) \simeq MU_0^2$. The solution is enabled by considering generalized time–space coordinates, $\bar{w} = \sum_{n=1}^{\infty} \phi_n(\bar{x}) \bar{q}_n(\bar{t})$, with $\phi_n(\bar{x}) = \sin(n\pi\bar{x})$ for a simply supported beam; that is

$$\left. \begin{aligned} \sum_{n=1}^{\infty} \left(\frac{d^2 \bar{q}_n}{d\bar{t}^2} + 2\pi^2 \zeta(\bar{t}) \frac{d\bar{q}_n}{d\bar{t}} + \alpha_n (n\pi)^4 \bar{q}_n(\bar{t}) \right) \phi_n(\bar{x}) &= 0 \\ \frac{d\zeta}{d\bar{t}} &= \frac{\Gamma}{2\pi^2} \left(\frac{T(\bar{t})}{T_0} - \frac{T_\infty}{T_0} \right); \quad \frac{T(\bar{t})}{T_0} = \frac{1}{2} \sum_{n=1}^{\infty} \left(\frac{d\bar{q}_n}{d\bar{t}} \right)^2 \\ \bar{q}_n(0) &= 0; \quad \frac{d\bar{q}_n}{d\bar{t}}(0) = \epsilon \frac{4 \sin^2(n\pi/2)}{n\pi}; \quad \zeta(0) = \zeta_0 \end{aligned} \right\} \quad (28)$$

where α_n is given by

$$\alpha_n = 1 - \frac{\bar{P}}{n^2} \quad (29)$$

It is well known, for the undamped system, that a load beyond the first Euler buckling load ($\alpha_1 < 0$)—within the assumption of small deformation—entails hyperbolic solutions and thus unstable motions in contrast to the bounded trigonometric solutions for $\alpha_n > 0$ (see e.g., Ref. [11]). The same holds true for a constant damping ratio. The question we want to address with this textbook example is whether the presence of a thermostat (and thus damping) can stabilize the motion and provide a means to evaluate stability or instability of the motion. With this focus in mind, we consider different constant load levels, beyond the first Euler buckling load $\bar{P} \in [1, 10]$. We consider an initial perturbation of $\epsilon = 10^{-5}$ and set the target temperature to $T_\infty/T_0 = 0$, with the expectation that this asymptotic temperature provides the highest level of damping.

The time-evolution of the kinetic temperature is shown in Fig. 5(a). It is characterized by three phases: an initial exponential increase of the kinetic temperature as one would expect from the dominance of the hyperbolic solutions; a kinetic temperature burst exhibiting a maximum; and a rapid descent to an (almost) constant asymptotic temperature well above the imposed target temperature $T_\infty/T_0 \rightarrow 0$. The asymptotic temperature in the dynamic buckling scales linearly with the applied buckling load in excess of the first Euler buckling load, and it is inverse proportional to the beam-to-bath mass ratio; that is

$$t \gg t_c : \frac{T}{T_0} \sim \frac{\bar{P} - 1}{\Gamma} \quad (30)$$

where t_c is the time at which the maximum temperature occurs and which scales for $T_\infty/T_0 \rightarrow 0$ approximately by

$$t_c \sim \frac{1}{\omega_0 \sqrt{\bar{P} - 1}} \left(1 + \frac{1}{a} \ln \frac{(\bar{P} - 1)}{\Gamma} \right) \quad (31)$$

with $a = 31.25$ obtained by fitting the results for a large range of (\bar{P}, Ω) values. Also shown in Fig. 5(a) is the divergence of the internal energy $U(\bar{t})/E_k(0)$ beyond the kinetic energy burst. The associated damping coefficient evolution shown in Fig. 5(b) is reminiscent of the kinetic temperature evolution, namely an exponential growth up to the peak temperature, followed by an (almost) linear increase associated with a nonzero constant asymptotic kinetic temperature, with a slope that scales as $d\bar{\zeta}/d\bar{t} \sim \bar{P} - 1$ (see Eqs. (27) and (30)). That is, the damping coefficient never reaches an asymptote.

The observation that the beam's kinetic temperature during buckling does not converge to the prescribed bath temperature (here $T_\infty/T_0 \rightarrow 0$) is indicative of the unstable nature of the problem. The instability of the motion herein identified may well be due to the limitations of the second-order beam theory considered in the potential energy expression (13) (for a discussion of higher order theories, see e.g., Ref. [10]). Yet, within the limits of the second-order theory employed, the nonconvergence of the kinetic temperature (Fig. 5(a)) means that the beam cannot establish an equilibrium state consistent with the prescribed bath temperature. In fact, from a statistical mechanics perspective, two systems are considered in thermodynamic equilibrium when they have the same temperature (see e.g., Ref. [5]). Unable to reach this equilibrium state, the beam's kinetic temperature cannot be sufficiently thermalized to stop the unstable motion by means of system dissipation, which is reflected by the divergence of the internal energy (Fig. 5(a)), and the unbounded increase of the damping coefficient (Fig. 5(b)). Otherwise said, the difference in kinetic temperature between beam and bath can serve as a straightforward stability criterion for stability-sensitive structures—without the need for further analysis of internal or potential energy.

4 Conclusions

It has thus been shown that the kinetic temperature of a structure is a useful quantity to explore the dynamic response of engineering structures. In this paper, we explore its application in structural dynamics through the proposition of a Nosé–Hoover beam theory:

- (1) Structural damping, that is the presence of a velocity dependent dissipative term in the equation of motion, can be rationalized as a thermalization process between a structure (here a beam) and an outside bath (understood in a broad sense as a system property). This is the fundamental idea of the Nosé–Hoover thermostat, which permits the analysis of a system in the canonical thermodynamic ensemble characterized asymptotically by a constant mean temperature, in contrast to the microcanonical ensemble characterized by a constant energy. While our developments limit themselves to the Nosé–Hoover thermostat, it should be noted that other thermostats exist that are frequently employed in molecular simulations, and which remain to be adapted to gain relevance in structural dynamics.
- (2) The Nosé–Hoover formalism well established for molecular systems is well adapted to structural elements of engineering structures. It consists of considering the sum of the Lagrangian (or Hamiltonian) of beam and bath, coupled by a heat exchange rate, the mass–damping coefficient. Instead of a constant damping, the Nosé–Hoover thermostat thus offers a new degree of freedom, namely a kinetic temperature dependent evolution of damping to ultimately reach the bath temperature at equilibrium. From eigen-vibration analysis, the commonality and differences of the Nosé–Hoover beam theory with constant mass damping models have been shown, which permit a handshake between the classical damping models and statistical mechanics–based thermalization models.

- (3) The solid foundation of these thermalization models in statistical physics provides new insights and stability criteria for engineering structures. This has been shown for the case of dynamic buckling, for which a steady-state difference in kinetic temperature between structure and bath provides a straightforward means to identify the beam as unstable—without the need for further analysis of internal or potential energy. It is expected that the kinetic temperature can serve as a structural order parameter to identify and comprehend failure of structures, well beyond elastic stability analysis considered here.

Acknowledgment

This research was carried out by the Concrete Sustainability Hub (CSHub@MIT), with funding provided by the Portland Cement Association (PCA) and the Ready Mixed Concrete Research & Education Foundation (RMC E&F). The CSHub@MIT is solely responsible for content. Additional support was provided by ICoME2 Labex (ANR-11-LABX-0053) and the A*MIDEX projects (ANR-11-IDEX-0001-02) cofunded by the French program “Investissements d’Avenir,” which is managed by the ANR, the French National Research Agency. The authors are grateful for fruitful discussions with Konstantinos Keremides (M.I.T.), Professor Mazdak Tootkaboni (Univ. of Massachusetts, Dartmouth), and Professor Mohammad Javad Abdolhosseini Qomi (Univ. of California, Irvine).

Appendix: Generalized Coordinates and Time Integration Scheme for Nosé–Hoover Beam Theory

The focus of this Appendix is twofold: (1) To show that a generalized coordinate solution is readily derived using the Nosé–Hoover extended system description; and (2) to specify the time integration scheme employed for the solution.

Consider thus generalized coordinates for the simple supported beam subject to eigen-vibrations

$$\begin{aligned} w\left(\bar{x} = \frac{x}{L}, \bar{t} = t\omega_0\right) &= \frac{V_0}{\omega_0} \sum_{n=1}^{\infty} \phi_n(\bar{x}) \bar{q}_n(\bar{t}) \\ &= \frac{V_0}{\omega_0} \sum_{n=1}^{\infty} \sin(n\pi\bar{x}) \bar{q}_n(\bar{t}) \end{aligned} \quad (A1)$$

The derivatives read

$$\frac{dw}{dt} = \omega_0 \frac{dw}{d\bar{t}} = V_0 \sum_{n=1}^{\infty} \phi_n(\bar{x}) \frac{d\bar{q}_n}{d\bar{t}} \quad (A2)$$

$$\frac{d^2w}{dx^2} = \frac{1}{L^2} \frac{d^2w}{d\bar{x}^2} = -\frac{V_0}{\omega_0 L^2} \sum_{n=1}^{\infty} (n\pi)^2 \phi_n(\bar{x}) \bar{q}_n(\bar{t}) \quad (A3)$$

Hence, the beam Lagrangian becomes when making use of the orthogonality of eigenmodes

$$\mathcal{L}_S = E_k(0) \left(\frac{1}{2} \sum_{n=1}^{\infty} \left(\frac{d\bar{q}_n}{d\bar{t}} \right)^2 - \left(\frac{1}{2} \sum_{n=1}^{\infty} (n\pi)^2 \bar{q}_n^2 \right) \right) \quad (A4)$$

where $E_k(0) = \rho ALV_0^2/2$ is the initial kinetic energy. Analogous to Eqs. (5) and (6), consider the Nosé–Hoover time shift relations and associated derivatives

$$\bar{\zeta} = \frac{ds}{d\tau}; \quad s = \frac{d\tau}{d\bar{t}} \omega_0; \quad \frac{\partial s}{\partial \bar{t}} = \frac{\bar{\zeta}s}{\omega_0} \quad (A5)$$

$$\frac{d\bar{q}_n}{d\bar{t}} = \frac{s}{\omega_0} \frac{\partial \bar{q}_n}{\partial \tau}; \quad \frac{d^2 \bar{q}_n}{d\bar{t}^2} = \frac{1}{\omega_0^2} \left(s^2 \frac{\partial^2 \bar{q}_n}{\partial \tau^2} + s\zeta \frac{\partial \bar{q}_n}{\partial \tau} \right) \quad (\text{A6})$$

The total Lagrangian of beam and bath, $\mathcal{L} = \mathcal{L}_S + \mathcal{L}_{Bath}$ (see Eq. (4)) thus reads:

$$\mathcal{L} = \frac{\rho ALV_0^2}{2} \left(\frac{1}{2} \left(\frac{s}{\omega_0} \right)^2 \sum_{n=1}^{\infty} \left(\frac{\partial \bar{q}_n}{\partial \tau} \right)^2 - \left(\frac{1}{2} \sum_{n=1}^{\infty} (n\pi)^2 \bar{q}_n^2 \right) \right) + \frac{1}{2} Q \zeta^2 - RT_{\infty} \ln(s) \quad (\text{A7})$$

We thus develop $n + 1$ Euler–Lagrange equation; first for \bar{q}_n

$$\begin{aligned} \forall n; \quad \frac{\partial \mathcal{L}}{\partial \bar{q}_n} &= \frac{\partial}{\partial \tau} \left(\frac{\partial \mathcal{L}}{\partial (\partial \bar{q}_n / \partial \tau)} \right) \\ &\Downarrow \\ -(n\pi)^2 \bar{q}_n &= \frac{1}{\omega_0^2} \left(s^2 \left(\frac{\partial^2 \bar{q}_n}{\partial \tau^2} \right) + 2\zeta s \frac{\partial \bar{q}_n}{\partial \tau} \right) \end{aligned} \quad (\text{A8})$$

and after transfer into real time

$$\forall n; \quad \frac{d^2 \bar{q}_n}{d\bar{t}^2} + \frac{\zeta(\bar{t})}{\omega_0} \frac{d\bar{q}_n}{d\bar{t}} + (n\pi)^2 \bar{q}_n = 0 \quad (\text{A9})$$

Second, the Euler–Lagrange equation for the Nosé–Hoover variable s and velocity $\xi = ds/d\tau$ reads here

$$\begin{aligned} \frac{\partial}{\partial \tau} \left(\frac{\partial \mathcal{L}}{\partial \xi} \right) &= \frac{\partial \mathcal{L}}{\partial s} \\ &\Downarrow \\ \frac{\partial \xi}{\partial \tau} Q &= \frac{\rho ALV_0^2}{2\omega_0^2} s \sum_{n=1}^{\infty} \left(\frac{\partial \bar{q}_n}{\partial \tau} \right)^2 - RT_{\infty} \frac{1}{s} \end{aligned} \quad (\text{A10})$$

Thus in time domain

$$\frac{\partial \xi}{\partial \bar{t}} = \frac{RT_0}{Q} \left(\frac{1}{2} \sum_{n=1}^{\infty} \left(\frac{d\bar{q}_n}{d\bar{t}} \right)^2 - \frac{T_{\infty}}{T_0} \right) \quad (\text{A11})$$

where we used $RT_0 = 2E_k(0) = \rho ALV_0^2$. Letting $\xi = (2\pi^2 \omega_0) \zeta$ in Eq. (A11) yields Eq. (17), with the kinetic temperature given in generalized coordinates by

$$\frac{T(\bar{t})}{T_0} = \frac{1}{2} \sum_{n=1}^{\infty} \left(\frac{d\bar{q}_n}{d\bar{t}} \right)^2 \quad (\text{A12})$$

Equation (A9) need to be solved, for all n , for the initial conditions

$$w(0) = 0;$$

$$\begin{aligned} \frac{dw}{d\bar{t}}(0) &= \frac{V_0}{\omega_0} \iff \frac{d\bar{q}_n}{d\bar{t}}(0) = \frac{\int_0^1 \phi_n(\bar{x}) d\bar{x}}{\int_0^1 \phi_n^2(\bar{x}) d\bar{x}} = \frac{4 \sin^2(n\pi/2)}{n\pi}; \\ \zeta(0) &= \zeta_0 \end{aligned} \quad (\text{A13})$$

Adopting an explicit time integration scheme comes to assume the damping as constant at time-step $i = \bar{t}_i / \Delta \bar{t}$ of time interval $\Delta \bar{t} = \bar{t}_i - \bar{t}_{i-1} = (t_i - t_{i-1}) \omega_0 \ll 2 / (n_{\max}^2 \pi)$ [with n_{\max} the maximum eigen-mode number considered in the superposition of eigen-modes]. Mode accelerations, velocities, and displacements are thus obtained by classical time integration

$$\forall n = 1, n_{\max};$$

$$\frac{d^2 \bar{q}_n}{d\bar{t}^2}(\bar{t}_i) = - \frac{\left(2\pi^2 \zeta(\bar{t}_{i-1}) + (n\pi)^4 \Delta \bar{t} \right) \frac{d\bar{q}_n}{d\bar{t}}(\bar{t}_{i-1}) + (n\pi)^4 \bar{q}_n(\bar{t}_{i-1})}{\left(1 + 2\pi^2 \zeta(\bar{t}_{i-1}) \Delta \bar{t} + (n\pi)^4 \left(\frac{\Delta \bar{t}^2}{2} \right) \right)} \quad (\text{A14})$$

$$\frac{d\bar{q}_n}{d\bar{t}}(\bar{t}_i) = \frac{d\bar{q}_n}{d\bar{t}}(\bar{t}_{i-1}) + \frac{d^2 \bar{q}_n}{d\bar{t}^2}(\bar{t}_i) \Delta \bar{t} \quad (\text{A15})$$

$$\bar{q}_n(\bar{t}_i) = \bar{q}_n(\bar{t}_{i-1}) + \frac{d\bar{q}_n}{d\bar{t}}(\bar{t}_{i-1}) \Delta \bar{t} + \frac{d^2 \bar{q}_n}{d\bar{t}^2}(\bar{t}_i) \frac{\Delta \bar{t}^2}{2} \quad (\text{A16})$$

The kinetic temperature at time \bar{t}_{i-1} is then obtained at the end of the time-step

$$\frac{T(\bar{t}_i)}{T_0} = \frac{1}{2} \sum_{n=1}^{n_{\max}} \left(\frac{d\bar{q}_n}{d\bar{t}}(\bar{t}_{i-1}) \right)^2 \quad (\text{A17})$$

together with the damping ratio:

$$\zeta(\bar{t}_i) = \zeta(\bar{t}_{i-1}) + \frac{d\zeta}{d\bar{t}}(\bar{t}_i) \Delta \bar{t} = \zeta(\tau_{i-1}) + \frac{\Delta \tau}{2\pi^2} \Gamma \left(\frac{T(\tau_i)}{T_0} \right) \quad (\text{A18})$$

A similar set of equations is readily developed for the dynamic buckling textbook example, requiring to modify the system of Eqs. (A13)–(A16) to account for the buckling load; that is, when considering the problem defined by Eq. (28)

$$\forall n = 1, n_{\max};$$

$$\frac{d^2 \bar{q}_n}{d\bar{t}^2}(\bar{t}_i) = - \frac{\left(2\pi^2 \zeta(\bar{t}_{i-1}) + (n\pi)^4 \Delta \bar{t} \right) \frac{d\bar{q}_n}{d\bar{t}}(\bar{t}_{i-1}) + \alpha_n (n\pi)^4 \bar{q}_n(\bar{t}_{i-1})}{\left(1 + 2\pi^2 \zeta(\bar{t}_{i-1}) \Delta \bar{t} + \alpha_n (n\pi)^4 \left(\frac{\Delta \bar{t}^2}{2} \right) \right)} \quad (\text{A19})$$

$$\frac{d\bar{q}_n}{d\bar{t}}(\bar{t}_i) = \frac{d\bar{q}_n}{d\bar{t}}(\bar{t}_{i-1}) + \frac{d^2 \bar{q}_n}{d\bar{t}^2}(\bar{t}_i) \Delta \bar{t} \quad (\text{A20})$$

$$\bar{q}_n(\bar{t}_i) = \bar{q}_n(\bar{t}_{i-1}) + \frac{d\bar{q}_n}{d\bar{t}}(\bar{t}_{i-1}) \Delta \bar{t} + \frac{d^2 \bar{q}_n}{d\bar{t}^2}(\bar{t}_i) \frac{\Delta \bar{t}^2}{2} \quad (\text{A21})$$

where $\alpha_n = 1 - \bar{P}/n^2$, with $\bar{P} = P/(\pi^2 EI/L^2)$ the axial load normalized by the first Euler buckling load.

References

- [1] Spence, S. M. J., and Kareem, A., 2014, “Tall Buildings and Damping: A Concept-Based Data-Driven Model,” *ASCE J. Struct. Eng.*, **140**(5), p. 04014005.
- [2] Pridham, B. A., and Wilson, J. C., 2004, “Identification of Base-Excited Structures Using Output-Only Parameter Estimation,” *Earthquake Eng. Struct. Dyn.*, **33**(1), pp. 133–155.
- [3] Hart, G. C., and Ibanez, G. C., 1973, “Experimental Determination of Damping in Nuclear Power Plant Structures and Equipment,” *Nucl. Eng. Des.*, **25**(1), pp. 112–125.
- [4] Adhikari, S., 2000, “Damping Models for Structural Vibration,” Ph.D. thesis, Cambridge University, Cambridge, UK.
- [5] Thorne, K. S., and Blandford, R. D., 2017, *Modern Classical Physics: Optics, Fluids, Plasmas, Elasticity, Relativity, and Statistical Physics*, Princeton University Press, Princeton NJ, Chap. 4.

- [6] Keremides, K., Qomi, M. J. A., Pellenq, R. J.-M., and Ulm, F.-J., 2018, "Potential-of-Mean-Force Approach for Molecular Dynamics-Based Resilience Assessment of Structures," *ASCE J. Eng. Mech.*, in Press.
- [7] Nosé, S., 1984, "A Unified Formulation of the Constant Temperature Molecular-Dynamics Methods," *J. Chem. Phys.*, **81**(1), pp. 511–519.
- [8] Hoover, W. G., 1985, "Canonical Dynamics: Equilibrium Phase-Space Distributions," *Phys. Rev. A*, **31**(3), pp. 1695–1697.
- [9] Huenenberger, P. H., 2005, "Thermostat Algorithms for Molecular Dynamics Simulations," *Adv. Polym. Sci.*, **173**, pp. 105–149.
- [10] Bazant, Z. P., and Cedolin, L., 1991, *Stability of Structures. Elastic, Inelastic, Fracture, and Damage Theories*, Oxford University Press, Oxford, UK.
- [11] Lindberg, H. E., 2003, *Little Book of Dynamic Buckling*, LCE Science/Software, Penn Valley CA.
- [12] Gladden, J. R., Handzy, N. Z., Belmonte, A., and Villiermaux, E., 2005, "Dynamic Buckling and Fragmentation in Brittle Rods," *Phys. Rev. Lett.*, **94**(3), p. 035503.